arXiv:0909.1584v1 [quant-ph] 8 Sep 2009

Optical Implementation of a Unitarily Correctable Code

K.M. Schreiter,[1,2] A. Pasieka,[3] R. Kaltenbaek,[1,2] K.J. Resch,[1,2] and D.W. Kribs[1,4]

[1] *Institute for Quantum Computing, University of Waterloo, Waterloo, Ontario, N2L 3G1, Canada*
[2] *Department of Physics & Astronomy, University of Waterloo, Waterloo, Ontario, N2L 3G1, Canada*
[3] *Department of Physics, University of Guelph, Guelph, Ontario, N1G 2W1, Canada*
[4] *Department of Mathematics & Statistics, University of Guelph, Guelph, Ontario, N1G 2W1, Canada*

(Dated: September 8, 2009)

Noise poses a challenge for any real-world implementation in quantum information science. The theory of quantum error correction deals with this problem via methods to encode and recover quantum information in a way that is resilient against that noise. Unitarily correctable codes are an error correction technique wherein a single unitary recovery operation is applied without the need for an ancilla Hilbert space. Here, we present the first optical implementation of a non-trivial unitarily correctable code for a noisy quantum channel with no decoherence-free subspaces or noiseless subsystems. We show that recovery of our initial states is achieved with high fidelity (≥ 0.97), quantitatively proving the efficacy of this unitarily correctable code.

PACS numbers: 42.50.Ex; 03.67.Pp; 03.67.Hk

I. INTRODUCTION

In the realm of quantum information science one of the most pervasive obstacles that must be overcome is the effect of interactions with the environment – the resulting noise must be dealt with in any quantum system of practical interest [1, 2]. The theory of quantum error correction has developed with this primary motivation in mind. The well-known passive error correction (or error avoidance) notions of decoherence-free subspaces (DFS) and noiseless subsystems (NS) [3, 4, 5, 6, 7, 8, 9] have been extensively explored. Experiments have demonstrated the principle of DFSs in optical systems [10, 11, 12], ion traps [13], and NMR [14]. The primary appeal of passive quantum error correction schemes is the fact they *are* passive – no correction operation is required once the noise acts. However, this occurs at the cost of a limited number of possible correctable codes for a given channel by relying heavily on symmetry in the noise [15].

When DFS/NS are not available or ideal, active quantum error correction (where a correction operation other than the identity map is needed) must be employed, resulting in an expanded set of correctable codes. Approaches such as the stabilizer formalism [16] provide formulas for finding and implementing codes in this regime. However, there can be a range of costs here that may negatively impact practical implementations. Clearly then, there are benefits to be had in the identification of correction schemes that require the application of a recovery operation, but retain some of the appealing properties of passive codes.

Here we experimentally implement a non-trivial example of such a correction scheme by applying random, anticorrelated noise to a two-qubit optical system. This noisy channel leads to the loss of encoded information and has no passive codes. However, we show that one qubit can be encoded against the noise such that the encoded states are recovered with high fidelity by applying a single unitary recovery operation after each application of the noisy channel. This form of *unitarily correctable code* was recently introduced [17, 18, 19].

II. UNITARILY CORRECTABLE CODES

One of the most general theoretical descriptions of how to deal with environmental interactions is given by the formalism of operator quantum error correction [17, 20]. In this theory, encoding, recovery and decoding of information takes place on subsystems of the full system. The key notion in operator quantum error correction is formulated as follows: a subsystem $\mathcal{H}^A$ of $\mathcal{H} = \left(\mathcal{H}^A \otimes \mathcal{H}^B\right) \oplus \mathcal{K}$ is *correctable* for a quantum channel $\mathcal{E}$ if there exists a recovery operation $\mathcal{R}$ such that for every pair of density operators $\rho^A \in \mathcal{H}^A$ and $\sigma^B \in \mathcal{H}^B$ there is some other density operator $\tau^B \in \mathcal{H}^B$ such that

$$\mathcal{R} \circ \mathcal{E} \circ \mathcal{P}_{AB}(\rho^A \otimes \sigma^B) = \mathcal{P}_{AB}(\rho^A \otimes \tau^B). \qquad (1)$$

Here $\mathcal{H}^B$ is an ancillary subsystem, $\mathcal{K}$ is an ancillary subspace orthogonal to $\mathcal{H}^A \otimes \mathcal{H}^B$, $\mathcal{P}_{AB}$ is the projection superoperator of $\mathcal{H}$ onto $\mathcal{H}^A \otimes \mathcal{H}^B$ and by a quantum channel, we refer to a completely-positive trace preserving map [1]. Simply stated, a subsystem $\mathcal{H}^A$ is correctable if, when we restrict our attention to it and anything it interacts with $(\mathcal{H}^A \otimes \mathcal{H}^B)$, there is a recovery operation that returns $\mathcal{H}^A$ to its initial state, while doing anything to $\mathcal{H}^B$.

Decoherence-free subspaces and noiseless subsystems are two special cases of Eq. (1), namely when the recovery operation is the identity map, and when $\dim \mathcal{H}^B = 1$ or $\dim \mathcal{H}^B \geq 1$ respectively. Active schemes such as the stabilizer formalism are examples of Eq. (1) in generality.

We say that a subsystem $\mathcal{H}^A$ is *unitarily correctable* for a quantum channel $\mathcal{E}$ if there exists a unitary recovery operation $\mathcal{U}$ such that for every pair of density operators $\rho^A \in \mathcal{H}^A$ and $\sigma^B \in \mathcal{H}^B$ there is some other density operator $\tau^B \in \mathcal{H}^B$ such that

$$\mathcal{U} \circ \mathcal{E} \circ \mathcal{P}_{AB}(\rho^A \otimes \sigma^B) = \mathcal{P}_{AB}(\rho^A \otimes \tau^B), \qquad (2)$$

where $\mathcal{U}$ is a unitary map such that $\mathcal{U} : \rho \mapsto U\rho U^\dagger$, with U a unitary operator on $\mathcal{H}^A \otimes \mathcal{H}^B$. In the general case of Eq. (1), every recovery operation $\mathcal{R}$ can be implemented via a unitary map on a (in general) larger Hilbert space [1]. Thus from another perspective, unitarily correctable codes are precisely the codes for which an extended Hilbert space is not required in the recovery process.

It may not be immediately apparent why this is advantageous as it is simply a special case of Eq. (1). The first point to recognize is that Eq. (2) is a generalization of the DFS/NS case since the identity map is a unitary map – thus the number of correction options for a given quantum channel will be at least as large. More importantly perhaps, quantum channels with *no* passive codes can gain *nearly*-passive correction options. Secondly, this potential increase in correction options comes only at the cost of applying a single unitary map after the noise and no measurements. Thanks to these two points, unitarily correctable codes take advantage of two of the most appealing aspects of both active and passive correction schemes – increased range of correction options and easily implemented correction.

From a practical standpoint, a correction scheme is only useful if one can find codes for which the scheme is capable of correcting a class of error operations of interest. In the case of unitarily correctable codes this can be achieved for the class of unital operations (those for which the identity operator is unaffected by the noise $\mathcal{E}(I) = I$) as shown by Theorem 2 of [18]. The theorem states that the unitarily correctable codes for a quantum channel $\mathcal{E}$ are precisely the DFS/NS for $\mathcal{E}^\dagger \circ \mathcal{E}$, where $\mathcal{E}^\dagger$ denotes the dual map for $\mathcal{E}$, defined via the relation between expectation values: $\mathrm{Tr}\left(\mathcal{E}(\rho)X\right) = \mathrm{Tr}\left(\rho\mathcal{E}^\dagger(X)\right)$. One can readily check that $\mathcal{E}$ is unital and trace preserving if and only if $\mathcal{E}^\dagger$ is as well.

The problem of finding the DFS/NS for a given channel has been fully characterized [15, 21]. In the case of a unital channel, the DFS/NS are the subsystems of the full Hilbert space that commute with each of the Kraus operators of the channel. This fact, together with Theorem 2 of [18] provides a way to compute the unitarily correctable codes for a given unital channel. The next section includes an explicit calculation for a specific example.

III. EXPERIMENTAL MODEL

As a demonstrative example, we seek a simple quantum channel with no DFS/NS but with a unitarily correctable code. To that end, consider the two-qubit phase-flip channel with Kraus operators $\left\{\frac{1}{\sqrt{2}}Z_1, \frac{1}{\sqrt{2}}Z_2\right\}$ where $Z_1 = \sigma_z \otimes I$ and $Z_2 = I \otimes \sigma_z$.

First note that there are no DFS/NS for this channel: $\mathcal{E}$ is a unital map so we must consider the operators that commute with both Z_1 and Z_2. In the standard basis,

$$Z_1 = \begin{pmatrix} 1 & 0 & 0 & 0 \\ 0 & 1 & 0 & 0 \\ 0 & 0 & -1 & 0 \\ 0 & 0 & 0 & -1 \end{pmatrix}$$

and,

$$Z_2 = \begin{pmatrix} 1 & 0 & 0 & 0 \\ 0 & -1 & 0 & 0 \\ 0 & 0 & 1 & 0 \\ 0 & 0 & 0 & -1 \end{pmatrix}.$$

Considering an arbitrary matrix in the Hilbert space, $M = (m_{i,j})$:

$$[Z_1, M] = \begin{pmatrix} 0 & 0 & 2m_{1,3} & 2m_{1,4} \\ 0 & 0 & 2m_{2,3} & 2m_{2,4} \\ -2m_{3,1} & -2m_{3,2} & 0 & 0 \\ -2m_{4,1} & -2m_{4,2} & 0 & 0 \end{pmatrix}. \quad (3)$$

The off-diagonal blocks must thus be equal to zero for any element of the Hilbert space to commute with Z_1 and so all elements of the Hilbert space that commute with Z_1 must be of the form (for arbitrary a through h):

$$\begin{pmatrix} a & b & 0 & 0 \\ c & d & 0 & 0 \\ 0 & 0 & e & f \\ 0 & 0 & g & h \end{pmatrix}.$$

Similarly, the elements that commute with Z_2 are:

$$\begin{pmatrix} j & 0 & k & 0 \\ 0 & l & 0 & m \\ n & 0 & o & 0 \\ 0 & p & 0 & q \end{pmatrix},$$

for arbitrary j through q. Therefore, the only operators that commute with both Z_1 and Z_2 are of the form

$$\begin{pmatrix} r & 0 & 0 & 0 \\ 0 & s & 0 & 0 \\ 0 & 0 & t & 0 \\ 0 & 0 & 0 & u \end{pmatrix},$$

for arbitrary r through u. Since there are no non-zero off-diagonal elements we cannot encode any quantum information – there are no DFS/NS for $\mathcal{E}$.

However, because $\mathcal{E}$ is a unital map we can find the unitarily correctable codes for $\mathcal{E}$ by looking at the DFS/NS for $\mathcal{E}^\dagger \circ \mathcal{E}$. The Kraus operators for the unital channel $\mathcal{E}^\dagger \circ \mathcal{E}$ are $\left\{\frac{1}{\sqrt{2}}I, \frac{1}{\sqrt{2}}Z_1Z_2\right\}$. In the standard basis

$$Z_1Z_2 = \begin{pmatrix} 1 & 0 & 0 & 0 \\ 0 & -1 & 0 & 0 \\ 0 & 0 & -1 & 0 \\ 0 & 0 & 0 & 1 \end{pmatrix},$$

thus the operators that commute with the Kraus operators of $\mathcal{E}^\dagger \circ \mathcal{E}$ are of the form

$$\begin{pmatrix} a & 0 & 0 & b \\ 0 & c & d & 0 \\ 0 & e & f & 0 \\ g & 0 & 0 & h \end{pmatrix},$$

for arbitrary a through h. So, there are two one-qubit unitarily correctable codes for $\mathcal{E}$ (the two one-qubit decoherence-free subspaces for $\mathcal{E}^\dagger \circ \mathcal{E}$): $\mathcal{C}_1 = \mathrm{span}(|00\rangle, |11\rangle)$ and $\mathcal{C}_2 = \mathrm{span}(|01\rangle, |10\rangle)$.

Finally, in order to find a suitable correction operation, consider the effect of $\mathcal{E}$ on an arbitrary two-qubit density matrix $\rho = (\rho_{i,j})$:

$$\mathcal{E}(\rho) = \begin{pmatrix} \rho_{1,1} & 0 & 0 & -\rho_{1,4} \\ 0 & \rho_{2,2} & -\rho_{2,3} & 0 \\ 0 & -\rho_{3,2} & \rho_{3,3} & 0 \\ -\rho_{4,1} & 0 & 0 & \rho_{4,4} \end{pmatrix}. \qquad (4)$$

There are many candidate unitary correction operations – for $\mathcal{C}_1$ the controlled-phase gate is one – it is also easy to see that both Z_1 and Z_2 will correct either of $\mathcal{C}_1$ or $\mathcal{C}_2$ when taken as the unitary matrix of Eq. (2). In any experimental setting, some gates are easier to implement than others (e.g. in the optical setting, 2-qubit gates are difficult because of the lack of photon-photon interactions). The flexibility in the choice of the unitary correction operation is another appealing aspect of unitarily correctable codes.

We have found what we set out to look for, a quantum channel with no DFS/NS, but two unitarily correctable codes. Although one qubit cannot be encoded with no recovery operation, one can be encoded with a single unitary recovery. Therefore this model allows for a clear experimental demonstration of one of the key advantages of the unitarily correctable code approach – we gain a *nearly-passive correction scheme* for a quantum channel with *no passive codes.*

An additional advantage of this model is that it can be realized in an optical setting. Defining $|H\rangle \equiv |0\rangle$ and $|V\rangle \equiv |1\rangle$, a phase-flip can be achieved by placing a half-wave plate (HWP) with its optic axis oriented along $|H\rangle$ in the path of a photon. Thus Z_1 (Z_2) is implemented by a HWP in the first (second) photon path with nothing in the second (first). Since both Z_1 and Z_2 will correct either codespace, we can experimentally implement the correction by placing a HWP in either photon path.

Thus, the particular optical implementation of the unitarily correctable code we consider is as follows: considering

$$\mathcal{U} \circ \mathcal{E} \circ \mathcal{P}_{AB}(\rho^A \otimes \sigma^B) = \mathcal{P}_{AB}(\rho^A \otimes \tau^B),$$

the full Hilbert space $\mathcal{H}$ is the set of polarization states of two entangled photons. $\mathcal{H}$ can be decomposed as $\mathcal{H} = (\mathcal{H}^A \otimes \mathcal{H}^B) \oplus \mathcal{K}$ where $\dim \mathcal{H}^B = 1$. The single encoded qubit will be supported on $P_{\mathcal{C}_1} = |00\rangle\langle 00| + |11\rangle\langle 11|$, so $\dim \mathcal{H}^A = 2$, and the ancilla space $\mathcal{K}$ is supported on $P_{\mathcal{C}_1^\perp} = |01\rangle\langle 01| + |10\rangle\langle 10|$ and also has dimension 2. Thus the projection superoperator $\mathcal{P}_{AB}$ focuses our attention onto the codespace $\mathcal{C}_1$: $\mathcal{P}_{AB} : \rho \mapsto P_{\mathcal{C}_1} \rho P_{\mathcal{C}_1}$. The noise is provided by randomly fired anti-correlated phase-flips in both photon paths and has the form $\mathcal{E} : \rho \mapsto \frac{1}{2} Z_1 \rho Z_1 + \frac{1}{2} Z_2 \rho Z_2$. Finally, the correction operation is provided by a single HWP placed in the second photon path, set to apply Z_2, so $\mathcal{U} : \rho \mapsto Z_2 \rho Z_2$.

IV. EXPERIMENTAL SETUP

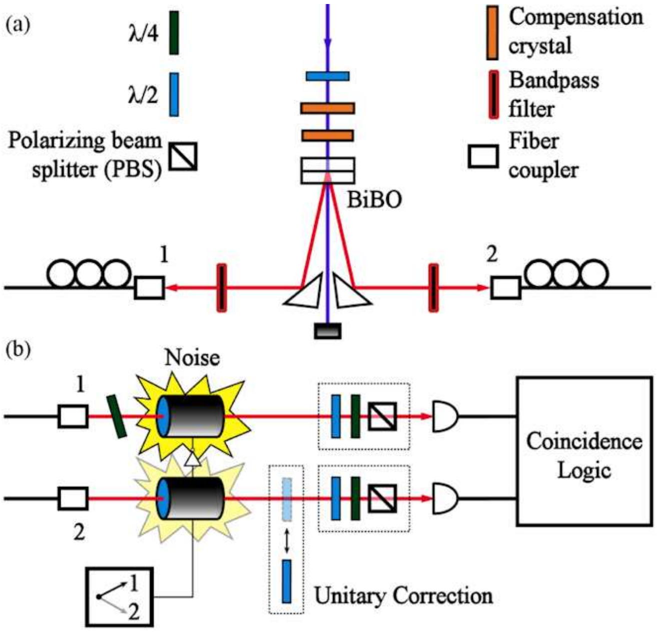

FIG. 1: (Color online) Experimental setup. (a) Source of polarization-entangled photon pairs. An ultraviolet diode laser is used to pump a pair of orthogonally-oriented BiBO crystals to produce entangled photon pairs by spontaneous parametric down-conversion. The precise state produced is determined by the polarization of the laser light and can be set using a half-wave plate (HWP). A pair of compensation crystals are used to compensate group-velocity mismatch in the down-conversion crystals. The light is collected into single-mode fibers. More details can be found in the text. (b) Experimental implementation of the noise model, correction, and tomography. A quarter-wave plate is used to adjust the phase of the entangled pairs; together with the HWP in the UV laser and the fiber-based polarization controllers, these operations are sufficient to prepare an arbitrary pure state in $\mathcal{C}_1$. When the noise is on, the photon pairs are subject to computer controlled anti-correlated phase errors through liquid-crystal variable phase retarders (LCVR); a decision as to which LCVR will fire is made by a pseudo-random number generator every 1 s. The state of the light is measured using quantum state tomography with a tomographically overcomplete set of measurements and the maximum likelihood procedure [22].

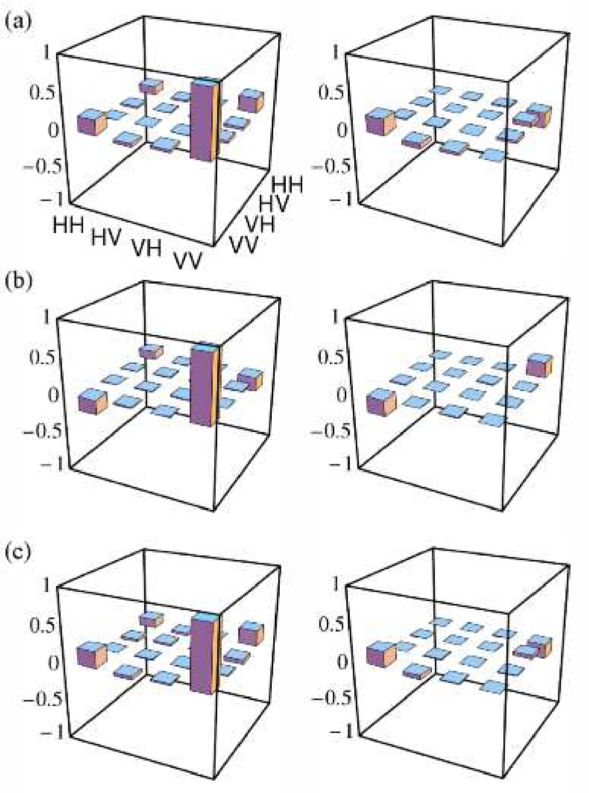

FIG. 2: (Color online) Example set of experimentally measured two-photon density matrices (left: real parts, right: imaginary parts). (a) The initial state was chosen to have a non-trivial value of both angles in Eq. (5); the nearest pure state in $\mathcal{C}_1$ has angles $\theta = 35.5°$ and $\phi = 46.5°$. (b) The noise affected state has its fidelity to the initial state reduced to 0.62; one can see that the primary effect of the noise is to flip the sign of the real and imaginary parts of the coherences rather than decohere the state. (c) The final state after both noise and correction. The fidelity with the initial state has been restored to 0.97 thus demonstrating the efficacy of the unitarily correctable code.

Our experimental source is shown in Fig. 1(a). We use a 185 mW free-running UV diode laser (Newport model: LQC405-180E, centre wavelength 404.4 nm, bandwidth 0.8 nm FWHM). To improve mode quality, the beam is passed through a spatial filter to obtain a 55 mW near-TEM$_{00}$ beam. A motorized half-wave plate then rotates the pump polarization from horizontal to an arbitrary linear polarization. The diode laser pumps a pair of 0.5 mm thick orthogonally-oriented BiBO nonlinear crystals cut for type-I non-collinear degenerate down-conversion with an 3° half-opening angle outside the crystal [23]. A 1 mm α-BBO and a 1 mm quartz both cut for maximum birefringence are used to compensate group-velocity mismatch in the down-conversion crystals. Entangled photon pairs emitted by the source pass through bandpass filters (centre wavelength 810 nm, bandwidth 5 nm FWHM) and are coupled into single-mode optical fibers.

The light is coupled back into free space before application of the noise, as shown in Fig. 1(b). The noise $\mathcal{E}$ is implemented by a pair of computer controlled liquid-crystal variable phase retarders (Meadowlark LVC-100, LCVR), one in each photon path. The LCVRs are both set to implement phase-flips. To simulate a noisy channel *either* one or the other LCVR is randomly fired with a switching rate of 1 Hz providing anti-correlated noise. The random switching was implemented using a software pseudo-random number generator (LabView, National Instruments). Recovery is achieved with a half-wave plate oriented along $|H\rangle$ in the path of photon 2.

We characterize all of our states using quantum state tomography, Fig 1(b). There is a polarization analyzer in each arm comprised of a half-wave plate, a quarter-wave plate, and a polarizing beam-splitter. We use the tomographically-overcomplete polarization measurements $\{H, V, D, A, R, L\}$ for each photon (R and L represent right- and left-circular polarizations), i.e., 36 measurement settings on the pair of photons. Density matrices are reconstructed from the experimentally measured counts using the maximum-likelihood method [22]. We performed quantum state tomography at each of three stages in the experiment: in the absence of noise or correction, in the presence of noise, and in the presence of both noise and correction.

Typical rates for the source are approximately 12000 coincidence counts/s and 60000 singles counts/s when the fibers are directly connected to detectors. Using the half-wave plate placed before the down-conversion crystals, the fiber-based polarization controllers, and the tilted quarter-wave plate in the path of photon 1, the source can produce output states in $\mathcal{C}_1$ of the form

$$|\psi\rangle = \cos 2\theta |HH\rangle + \sin 2\theta e^{i\phi} |VV\rangle. \tag{5}$$

With the half-wave plate oriented at $\theta = 22.5°$ and the phase angle at $\phi = 0$ the system ideally produces the Bell state $|\phi^+\rangle = \frac{1}{\sqrt{2}}(|HH\rangle + |VV\rangle)$. In this case, we measure visibilities of 99.2% in the horizontal/vertical (H/V) basis and 95.3% in the diagonal/antidiagonal (D/A) basis. Reconstructing the state using quantum state tomography we find, in this case, that the fidelity [24, 25] with $|\phi^+\rangle$ is 0.97, the tangle [26] is $\tau = 0.9$, and the linear entropy [27] is $S_L = 0.065$. Thus our source is capable of producing highly entangled and nearly pure states.

V. RESULTS & DISCUSSION

An example set of reconstructed density matrices, chosen to show the effect of the noise and correction on a state with unequal populations, and both real and imaginary coherences, is shown in Fig. 2. Data was accumulated for 5 s per measurement setting. The initial state is shown in Fig. 2(a). This state has fidelity 0.98 with a state in $\mathcal{C}_1$ [Eq. (5)] with $\theta = 35.5°$ and $\phi = 46.5°$. Subjecting the photon pairs to the noise changes the state

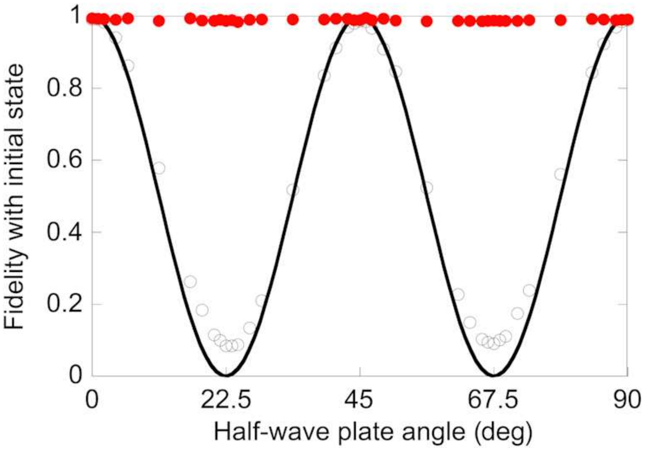

FIG. 3: (Color online) Measured fidelity between initial and final states. The mixed state fidelity [24] was calculated on experimentally reconstructed density matrices between the initial states and noise-affected states (open circles, solid line theory) and the initial states and states affected by noise and unitary correction (closed, red circles). The data show that the effect of the noise depends strongly on the initial state. Initial states closest to the product states $|HH\rangle$ and $|VV\rangle$ are least affected while those close to the maximally entangled state $|\phi^+\rangle$ are driven to nearly orthogonal states. The correction restores the photons to states with fidelity of higher than 0.98 with the initial states in all cases.

to the one shown in Fig. 2(b). The fidelity of this state to the initial state in Fig. 2(a) has been reduced to 0.62. Qualitatively, one can see that the effect of the noise $\mathcal{E}$ does not decohere these states, but rather flips the sign of both the real and imaginary coherences. The correction, $\mathcal{U}$, is implemented by placing a half-wave plate in the path of photon 2. When the noisy state was corrected, we obtained the state shown in Fig. 2(c) where the fidelity with the initial state has been restored to 0.97. The recovery of high fidelity states demonstrates the effectiveness of this unitarily correctable code.

We characterized the effect of the noise and noise plus correction on a range of input states. We adjusted the source to states in $\mathcal{C}_1$ with real coefficients ($\phi = 0$) and tuned those coefficients by adjusting the angle of the HWP in the pump laser, θ. The fidelity measurements of the noise affected states are shown in Fig. 3 where the initial states are shown as open circles and the theoretical prediction, $F = \cos^2 4\theta$, is a solid black line. These data clearly show that the noise affects the states, but by different amounts. As expected, those states closer to the product states $|HH\rangle$ and $|VV\rangle$, or HWP settings 0° (or 90°) and 45°, respectively, are less affected by the noise; in the case of $|HH\rangle$ and $|VV\rangle$, the states are invariant under the noise. Those states closer to the maximally entangled states $|\phi^+\rangle$ and $|\phi^-\rangle = \frac{1}{\sqrt{2}}(|HH\rangle - |VV\rangle)$, or HWP settings 22.5° and 67.5°, respectively, are most affected by the noise as it drives them to nearly orthogonal states. The states are restored to greater than 0.98 fidelity in all measurements thereby demonstrating the effectiveness of this unitarily correctable code across the entire codespace $\mathcal{C}_1$.

VI. CONCLUSION

We have described a simple noise model which does not have a decoherence-free subspace or noiseless subsystem but does contain two unitarily correctable codes. We have implemented this noise model by constructing a quantum channel in a physical system, namely the polarization of a pair of optical photons, in which two liquid-crystal variable phase retarders fire in an anticorrelated, but random manner. We have sent photon pairs through this noisy channel in states ranging from separable to nearly maximally entangled and compared the impact of the noise and the noise plus unitary correction on the quality of the states. Our data shows that the noise can dramatically impact the fidelity of the output state with the initial, especially in the case of highly entangled states in $\mathcal{C}_1$. However, the unitary correction restores the state quality with fidelities greater than 0.97 for all states in $\mathcal{C}_1$.

Our experiment shows how to translate the theory of unitarily correctable codes, a new method combining aspects of passive and active quantum error correction, into experimental realization. As these codes expand the class of nearly-passive correctable codes, it is an interesting open question as to how these approaches could be utilized in more natural physical systems, as opposed to controlled application of noise.

VII. ACKNOWLEDGMENTS

This work was funded by NSERC, Ontario MRI ERA, CFI, IQC, and OCE. A.P. was partially supported by an Ontario Graduate Scholarship. R.K. acknowledges financial support from IQC. We thank Zhenwen Wang for technical assistance with electronics.

---

[1] M. A. Nielsen and I. L. Chuang, *Quantum Computation and Quantum Information* (Cambridge, New York, 2000).

[2] D. Gottesman, Quantum error correction and fault tolerance, in *Encyclopedia of Mathematical Physics*, edited by J.-P. Francoise, G. Naber, and S. Tsou Vol. 4, p. 196, Oxford, Elsevier, 2006, quant-ph/0507174.

[3] G. Palma, K.-A. Suominen, and A. Ekert, Proc. R. Soc.

Lond. A **452**, 567 (1996), quant-ph/9702001.

[4] L.-M. Duan and G.-C. Guo, Phys. Rev. Lett. **79**, 1953 (1997), quant-ph/9703040.

[5] P. Zanardi and M. Rasetti, Phys. Rev. Lett. **79**, 3306 (1997), quant-ph/9705044.

[6] D. Lidar, I. Chuang, and K. Whaley, Phys. Rev. Lett. **81**, 2594 (1998), quant-ph/9807004.

[7] E. Knill, R. Laflamme, and L. Viola, Phys. Rev. Lett. **84**, 2525 (2000), quant-ph/9908066.

[8] P. Zanardi, Phys. Rev. A **63**, 012301 (2000), quant-ph/9910016.

[9] J. Kempe, D. Bacon, D. A. Lidar, and K. B. Whaley, Phys. Rev. A **63**, 42307 (2001), quant-ph/0004064.

[10] P. G. Kwiat, A. J. Berglund, J. B. Altepeter, and A. G. White, Science **290**, 498 (2000).

[11] M. Mohseni, J. S. Lundeen, K. J. Resch, and A. M. Steinberg, Phys. Rev. Lett. **91**, 187903 (2003), quant-ph/0212134.

[12] K. Banaszek, A. Dragan, W. Wasilewski, and C. Radzewicz, Phys. Rev. Lett. **92**, 257901 (2004), quant-ph/0403024.

[13] D. Kielpinski *et al.*, Science **291**, 1013 (2001).

[14] J. E. Ollerenshaw, D. A. Lidar, and L. E. Kay, Phys. Rev. Lett. **91**, 217904 (2003), quant-ph/0302175.

[15] M.-D. Choi and D. W. Kribs, Phys. Rev. Lett. **96**, 050501 (2006), quant-ph/0507213.

[16] D. Gottesman, Phys. Rev. A **54**, 1862 (1996), quant-ph/9604038.

[17] D. W. Kribs, R. Laflamme, D. Poulin, and M. Lesosky, Quantum Inf. Comput. **6**, 382 (2006), quant-ph/0504189.

[18] D. W. Kribs and R. W. Spekkens, Phys. Rev. A **74**, 042329 (2006), quant-ph/0608045.

[19] D. W. Kribs, A. Pasieka, and K. Zyczkowski, Open Syst. Inf. Dyn. **15**, 329 (2008), arXiv:0811.1621.

[20] D. Kribs, R. Laflamme, and D. Poulin, Phys. Rev. Lett. **94**, 180501 (2005), quant-ph/0412076.

[21] D. W. Kribs, Proc. Edinb. Math. Soc. **46**, 421 (2003), math/0309390.

[22] D. James, P. Kwiat, W. Munro, and A. White, Phys. Rev. A **64**, 052312 (2001), quant-ph/0103121.

[23] P. Kwiat, E. Waks, A. White, I. Appelbaum, and P. Eberhard, Phys. Rev. A **60**, R773 (1999), quant-ph/9810003.

[24] R. Jozsa, J. Modern Opt. **41**, 2315 (1994).

[25] The mixed state fidelity is $F = \left[\mathrm{Tr}\sqrt{\sqrt{\rho_1}\rho_2\sqrt{\rho_1}}\right]^2$.

[26] V. Coffman, J. Kundu, and W. K. Wootters, Phys. Rev. A **61**, 052306 (2000), quant-ph/9907047.

[27] Linear entropy is a measure of the purity of a quantum state ranging from 0 for pure states to 1 for maximally mixed states. For two qubits, it is defined $S_L = \frac{4}{3}(1 - Tr\rho^2)$.